

## Journal Pre-proofs

Research papers

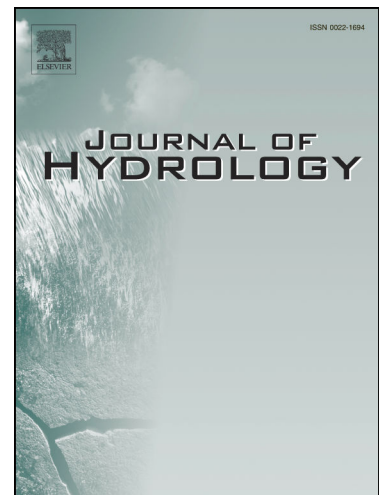
Parameterization of a comprehensive explicit model for single-ring infiltration

M. Iovino, M.R. Abou Najm, R. Angulo-Jaramillo, V. Bagarello, M. Castellini, P. Concialdi, S. Di Prima, L. Lassabatere, R.D. Stewart

PII: S0022-1694(21)00851-9

DOI: <https://doi.org/10.1016/j.jhydrol.2021.126801>

Reference: HYDROL 126801



To appear in: *Journal of Hydrology*

Received Date: 11 May 2021

Revised Date: 2 August 2021

Accepted Date: 5 August 2021

Please cite this article as: Iovino, M., Abou Najm, M.R., Angulo-Jaramillo, R., Bagarello, V., Castellini, M., Concialdi, P., Di Prima, S., Lassabatere, L., Stewart, R.D., Parameterization of a comprehensive explicit model for single-ring infiltration, *Journal of Hydrology* (2021), doi: <https://doi.org/10.1016/j.jhydrol.2021.126801>

This is a PDF file of an article that has undergone enhancements after acceptance, such as the addition of a cover page and metadata, and formatting for readability, but it is not yet the definitive version of record. This version will undergo additional copyediting, typesetting and review before it is published in its final form, but we are providing this version to give early visibility of the article. Please note that, during the production process, errors may be discovered which could affect the content, and all legal disclaimers that apply to the journal pertain.

© 2021 Published by Elsevier B.V.

# Parameterization of a comprehensive explicit model for single-ring infiltration

Iovino M.<sup>1\*</sup>, Abou Najm M.R.<sup>2</sup>, Angulo-Jaramillo R.<sup>3</sup>, Bagarello V.<sup>1</sup>, Castellini M.<sup>4</sup>, Concialdi P.<sup>1</sup>, Di Prima S.<sup>5</sup>, Lassabatere L.<sup>3</sup>, Stewart R.D.<sup>6</sup>

<sup>1</sup> Department of Agricultural, Food and Forest Sciences, University of Palermo, Viale delle Scienze, 90128 Palermo, Italy

<sup>2</sup> Department of Land, Air and Water Resources, University of California, Davis, CA 95616, United States

<sup>3</sup> Université de Lyon; UMR5023 Ecologie des Hydrosystèmes Naturels et Anthropisés, CNRS, ENTPE, Université Lyon 1, Vaulx-en-Velin, France

<sup>4</sup> Council for Agricultural Research and Economics - Agriculture and Environment Research Center (CREA-AA), Via Celso Ulpiani 5, 70125 Bari, Italy

<sup>5</sup> Department of Agricultural Sciences, University of Sassari, Viale Italia, 39, 07100 Sassari, Italy

<sup>6</sup> School of Plant and Environmental Sciences, Virginia Polytechnic Institute and State University, Blacksburg, VA, United State.

\* Corresponding Author: massimo.iovino@unipa.it

## ABSTRACT

Comprehensive infiltration models can simultaneously describe transient and steady-state infiltration behaviors, and therefore can be applied to a range of experimental conditions. However, satisfactory model accuracy requires proper parameterization, including estimating the transition time from transient to steady-state flow conditions ( $\tau_{crit}$ ). This study focused on improving the estimation of two parameters –  $\tau_{crit}$  and a second constant called  $a$  – used in a comprehensive, explicit, two-term model for single ring infiltration (hereafter referred to as the SA model). Different studies have recommended that  $a$  should be as low as 0.45 to as high as 0.91. Furthermore,  $\tau_{crit}$  is often obtained a-priori by assuming that steady-state conditions are reached before the end of an infiltration run. However, there has not been a systematic analysis of those terms for different soils and infiltration conditions. To investigate these open issues related to the use of the SA model, here we introduce a novel, iterative method for estimating  $\tau_{crit}$  and the parameter  $a$ . We then applied this method to both analytical and experimental infiltration data, and compared it with two existing empirical methods. The analytical infiltration experiments showed that  $\tau_{crit}$  was approximately 1.5 times larger than the maximum validity time of a similar two-term

transient infiltration model. Further, the iterative method for obtaining  $\tau_{crit}$  had minimal effects on the  $a$  term, which varied between 0.706 and 0.904 and was larger for finer soils and when small water sources were used. Application of the proposed method was less efficient with experimental data. Only ~33% of the experiments yielding plausible estimates of  $a$  (i.e.,  $a < 1$ ), indicating that these infiltration model parameters often have high uncertainty. The successful runs indicated that  $a$  depended on the rate at which the initial infiltration rate approached the final infiltration rate. Depending on the fitting algorithm used,  $a$  had mean values of 0.74 – 0.78, which were intermediate between those suggested by previous studies. Altogether, these findings expand the applicability of the SA model by providing new methods for estimating  $\tau_{crit}$  and by showing that  $a$  does not need to be fixed a-priori. We expect that these advances will result in more reliable estimations of soil hydrodynamic parameters, including hydraulic conductivity.

Keywords: Single ring infiltrometer, infiltration model parameterization, transition time

## INTRODUCTION

Field infiltration experiments are often used to determine soil saturated hydraulic conductivity,  $K_s$ , or near-saturated variations with minimum disturbance to the sampled soil volume (Angulo-Jaramillo et al., 2016; Bouma, 1982). Single ring infiltration tests offer the advantages of being easy to conduct and requiring minimal and inexpensive equipment. Three-dimensional flow from a single ring can be simulated by numerically solving the axisymmetric Richards equation with finite element codes (e.g., Šimůnek et al., 2018). However, estimating soil hydraulic parameters from numerical inversion of infiltrometer experiments is cumbersome and may experience a number of problems related to computational efficiency, convergence, and parameter uniqueness (Lazarovitch et al., 2007; Russo et al., 1991). Explicit solutions that account for three-dimensional flow paths in the soil are thus preferred for interpreting infiltration from a single ring source (Dohnal et al., 2016; Smith et al., 2002). Many formulations describe three-dimensional flow using the so-called  $\alpha^*$  parameter, which is often considered the reciprocal of soil macroscopic capillary length,  $\lambda$ , (Reynolds and Elrick, 2002).

At the same time, infiltration solutions need to account for the different phases of typical infiltration processes, which progress from an initial transient phase to a subsequent steady-state phase. Some models, e.g., Reynolds and Elrick (1990), determine  $K_s$  from three-dimensional, steady, ponded flow out of the ring. These approaches require reliable steady-state infiltration rate data, which can be impractical in some cases if the equilibration time is particularly long (Bagarello et al., 2019). By contrast, models that make use of the transient stage of the infiltration process overcome

uncertainties about the time at which steady-state flux is attained. Their interpretation allows for shorter experiments and smaller sampled volumes of soil, which provides better agreement with the hypotheses of homogeneity and initial uniform water content assumed by infiltration models (Di Prima et al., 2016; Vandervaere et al., 2000). However, these transient approaches require accurate measurement in the early stage of infiltration, which can be challenging under specific field conditions such as highly permeable, slightly sorptive and water-repellent soils (Di Prima et al., 2019).

The limitations associated with models focused exclusively on transient or steady-state behaviors has led to the development of several comprehensive models that can be applied under different infiltration stages (i.e. from early time to steady state conditions) and various initial and boundary conditions at the soil surface. One of the earliest comprehensive models for three-dimensional cumulative infiltration,  $I$ , vs. time,  $t$ , from a disk source into an initially unsaturated soil was proposed by Haverkamp et al. (1994). This solution is valid for any infiltration time, but can be complex to apply due to its implicit form. Its explicit expansions, valid for transient and steady-state infiltration stages, have successively been applied in a procedure known as Beerkan Estimation of Soil Transfer (BEST) parameters (Lassabatere et al., 2006), which allows a complete soil hydraulic characterization from a single ring infiltration test complemented by some basic soil physical characterization. One limitation of the Haverkamp model is that it was developed for tension infiltrometers, where the surface pressure head is less than or equal to zero and the disk source rests on the soil surface, making it less accurate in situation where source pressure head or ring insertion depths are positive (Stewart and Abou Najm, 2018a). The Haverkamp model also is only strictly valid under relatively dry initial soil water contents, i.e. the ratio of initial soil water content to saturated water content below 0.25.

Wu et al. (1999) proposed a generalized solution to infiltration from single-ring pressure infiltrometers which removed the requirements of steady-state and allowed estimation of  $K_s$  from the whole  $I(t)$  curve without assuming a pre-established value of the soil macroscopic capillary length or  $\alpha^*$  parameter. Building on the Wu et al. (1999) and Reynolds and Elrick (1990) solutions, Stewart and Abou Najm (2018a,b) developed a comprehensive infiltration model (SA model) for single ring source that appears to be particularly flexible as compared to other models. Specifically, it accounts for different ring sizes and depths of insertion, initial water contents, transient and steady-state infiltration behavior, and non-zero water supply pressures. However, the SA model uses a scaling parameter, referred to “ $a$ ”, whose exact value is subject to some debate. For example, Wu and Pan (1997) fitted a dimensionless infiltration equation to the numerically simulated single-ring infiltration data for three representative soils (sand, clay, sandy-clay-loam) and obtained  $a =$

0.91, a value that was subsequently used in an infiltration model by Wu et al. (1999). By analogy with Philip (1990), Stewart and Abou Najm (2018a) suggested that  $a$  should instead be equal to 0.45, i.e., approximately one half of the value recommended by Wu and Pan (1997). Those authors included a sensitivity analysis as on the  $a$  parameter, which showed that  $a$  varies between different soil types and initial water contents. These different recommendations and results imply that the  $a$  parameter warrants further investigation.

At the same time, application of either the SA model or the Haverkamp model requires estimates for the timescales over which the transient infiltration solutions are valid. In the SA model, the transition time is defined by  $\tau_{crit}$ , which was specified by Stewart and Abou Najm (2018a) to ensure continuity in the expressions for both infiltration rates and cumulative infiltration amounts. The Haverkamp model defines a slightly different term  $t_{max}$ , which represents the maximum time over which the transient solution applies. Both terms can be analytically defined (see Theory), and moreover, for null pressure head at the infiltration surface and depth of ring insertion equal to zero, the SA model and the explicit expansion of the Haverkamp model describe the same process and, thus, can be compared to identify the relationship between  $\tau_{crit}$  and  $t_{max}$ .

Identifying  $\tau_{crit}$  and  $t_{max}$  based on infiltration measurements poses a related set of challenges, as the parameters required to estimate these timescales are typically unknown a-priori. Assuming the steady-state conditions are reached before the end of an infiltration run, Di Prima et al. (2019) estimated the transition time as the first value for which linear regression line conducted for the last three  $I(t)$  data points deviates from the measured cumulative infiltration by a fixed threshold, often fixed at 2% following Bagarello et al. (1999). This approach may introduce considerable uncertainty in cases where steady-state conditions have not actually been met, thus warranting more study of this estimation approach. Furthermore, this method may identify  $\tau_{crit}$  values, and by extension infiltration model parameters, that violate the requirement that infiltration rate be continuous between the transient and steady-state phases.

This study investigates three open issues related to the use of the SA model for single ring infiltration: 1) how comparable is  $\tau_{crit}$  with the maximum time,  $t_{max}$ ? 2) how sensitive is  $\tau_{crit}$  to the empirical criterion used to fit it? 3) how does the scaling parameter  $a$  depend on different experimental conditions and can it be related to the parameters of Haverkamp model? To answer these questions, we applied an optimization procedure with a constraint among the infiltration coefficients to fit the SA model to both analytical and experimental infiltration data. We used that procedure to derive  $\tau_{crit}$  and the associated value of  $a$  for each infiltration process. The outcomes of proposed approach, which involves a simultaneous and coherent use of both transient and steady-

state infiltration data, is then discussed on the basis of theoretical considerations and comparison with simplified approaches to estimate the transition time.

## THEORY

### Infiltration model

Stewart and Abou Najm (2018a), building on the Wu et al. (1999) and Reynolds and Elrick (1990) solutions, developed the following explicit expressions of transient and steady-state three-dimensional (3D) cumulative infiltration,  $I$  (L), from a surface circular source under a positive pressure head:

$$I = \sqrt{\frac{(\theta_s - \theta_i)(h_{source} + \lambda)K_s}{b}} \sqrt{t} + a f K_s t \quad t < \tau_{crit} \quad (1a)$$

$$I = \frac{(\theta_s - \theta_i)(h_{source} + \lambda)}{4 f b (1 - a)} + f K_s t \quad t \geq \tau_{crit} \quad (1b)$$

$$\tau_{crit} = \frac{(\theta_s - \theta_i)(h_{source} + \lambda)}{4 b K_s f^2 (1 - a)^2} \quad (1c)$$

where  $t$  (T) is the time,  $\tau_{crit}$  (T) is the time of transition between early-time and steady-state infiltration behaviors,  $\theta_s$  ( $L^3 L^{-3}$ ) and  $\theta_i$  ( $L^3 L^{-3}$ ) are the respective saturated and initial volumetric soil water contents,  $h_{source}$  (L) is the established ponded depth of water on the infiltration surface,  $\lambda$  (L) is the macroscopic capillary length of the soil,  $K_s$  ( $L T^{-1}$ ) is the saturated soil hydraulic conductivity,  $a$  and  $b$  are dimensionless constants (with  $b \approx 0.55$ ; White and Sully, 1987), and  $f$  is a dimensionless correction factor that depends on soil initial and boundary conditions and ring geometry:

$$f = \frac{h_{source} + \lambda}{d + r_d / 2} + 1 \quad (2)$$

where  $d$  (L) is the depth of ring insertion and  $r_d$  (L) is the radius of the ring. The macroscopic capillary length,  $\lambda$ , is a measure of the soil capillary force. It is defined as the matrix flux potential,  $\phi$  ( $L^2 T^{-1}$ ), scaled by the difference between  $K_s$  and the soil hydraulic conductivity,  $K_i$  ( $L T^{-1}$ ), corresponding to the initial soil water pressure head,  $h_i$  (L):

$$\lambda = \frac{\phi}{\Delta K} = \frac{1}{K_s - K_i} \int_{h_i}^0 K(h) dh \quad (3).$$

Larger values of  $\lambda$  indicate greater contribution of the capillary forces relative to gravity. The  $\tau_{crit}$  time in Eq.(1c) is defined as the time when the infiltration rate ( $dI/dt$ ) is equal between Eqs.(1a) and (1b).

165 A general form of Eq.(1) can be written as follows:

$$166 \quad I = c_1\sqrt{t} + c_2t \quad t < \tau_{crit} \quad (4a)$$

$$167 \quad I = c_3 + c_4t \quad t \geq \tau_{crit} \quad (4b)$$

$$168 \quad \tau_{crit} = \frac{1}{4} \left( \frac{c_1}{c_4 - c_2} \right)^2 \quad (4c)$$

169 where the infiltration coefficients  $c_1$  (L T<sup>-0.5</sup>) and  $c_2$  (L T<sup>-1</sup>) can be determined by fitting Eq.(4a) to  
 170 the data corresponding to the transient time, and the intercept,  $c_3$  (L), and the slope,  $c_4$  (L T<sup>-1</sup>), of  
 171 Eq.(4b) can be estimated by linear regression analysis of the  $I$  vs.  $t$  data points associated with  
 172 steady-state conditions. To ensure continuity of cumulative infiltration,  $I$ , between Eqs.(4a) and (4b)  
 173 at  $t = \tau_{crit}$ , the following constraint should be placed among the four infiltration coefficients:

$$174 \quad c_3 = \frac{c_1^2}{4(c_4 - c_2)} = \tau_{crit} (c_4 - c_2) \quad \text{with } c_4 > c_2 \quad (5).$$

175 Here, we propose a novel and simple method for direct estimation of  $a$  from a single-ring  
 176 experiment that includes both the transient and the steady-state phases of the infiltration process. In  
 177 particular, the  $a$  constant can be derived from the parameterization of the infiltration coefficients  $c_2$   
 178 and  $c_4$  via:

$$179 \quad \frac{c_2}{c_4} = \frac{a f K_s}{f K_s} = a \quad (6).$$

180 The  $a$  constant thus quantifies the weight of conductivity part of infiltration equation in the transient  
 181 state ( $c_2$ ) as a proportion of that in the steady state condition ( $c_4$ ). Note that the condition  $c_4 > c_2$ ,  
 182 stated in Eq.(5), indicates that  $a$  should be  $< 1$  to be physically plausible or that the conductivity  
 183 weight is higher at the steady state than under transient conditions.

184

#### 185 **Investigation of $a=c_2/c_4$ ratio with the approach by Haverkamp et al. (1994)**

186 Haverkamp et al. (1994) proposed a set of two-term expansions for transient and steady-state  
 187 infiltration from a circular source, which are conceptually and functionally similar to Eqs.(1a) and  
 188 (1b):

$$189 \quad I(t) = c_1\sqrt{t} + c_2t = S\sqrt{t} + \left( \frac{2-\beta}{3}\Delta K + K_i + \frac{\gamma S^2}{r_d\Delta\theta} \right)t \quad t < t_{max} \quad (7a)$$

$$190 \quad I(t) = c_3 + c_4t = \frac{1}{2(1-\beta)} \ln\left(\frac{1}{\beta}\right) \frac{S^2}{\Delta K} + \left( K_s + \frac{\gamma S^2}{r_d\Delta\theta} \right)t \quad t > t_{max} \quad (7b)$$

191 in which  $S$  (L T<sup>-1/2</sup>) is the soil sorptivity,  $\beta$  and  $\gamma$  are infiltration constants that are usually fixed at  $\beta$   
 192  $= 0.6$  and  $\gamma = 0.75$ , and  $t_{max}$  (T) is the maximum time for which the transient expansion can be  
 193 considered valid (Lassabatere et al., 2006). Unlike the SA model, however, the two expressions of



Eq.(7) asymptotically approach the quasi-exact infiltration solution but are not considered valid at  $t = t_{max}$ . Thus, a discontinuity between the two equations is expected at  $t = t_{max}$  (Lassabatere et al., 2009; Angulo-Jaramillo et al., 2019). Nonetheless, this formulation is useful for exploring the validity of estimating  $a$  based on the ratio of the infiltration terms that scale linearly with time  $t$ . Specifically, substituting coefficients  $c_2$  and  $c_4$  of Eq.(7) into Eq.(6), and using the White and Sully (1987) expression for  $S$ , the following relationship for  $a$  is obtained:

$$a = \frac{\left(\frac{2-\beta}{3}\Delta K + K_i + \frac{\gamma\lambda}{br_d}\right)}{\left(K_s + \frac{\gamma\lambda}{br_d}\right)} \quad (8).$$

Assuming that  $K_i \approx 0$ , which is the case for most applications of the model (when  $\theta_i \leq 0.25 \theta_s$ ), and considering that Stewart and Abou Najm (2018a) showed that  $\lambda$  remained constant with  $\lambda \approx \lambda_{max}$  for initial degrees of saturation lower than 0.4, the following expression for  $a$  can be obtained:

$$a = \frac{\left(\frac{2-\beta}{3}K_s + \frac{\gamma\lambda_{max}}{br_d}\right)}{\left(K_s + \frac{\gamma\lambda_{max}}{br_d}\right)} \quad (9).$$

Eq.(9) shows that the value of  $a$  depends on the soil type ( $K_s$ ,  $\lambda_{max}$ ) and ring radius ( $r_d$ ), as well as on the values of the infiltration constants  $\beta$  and  $\gamma$ . In particular, for small ring radii or soils with high capillarity (e.g., fine-textured soils), the term  $\gamma\lambda_{max}/br_d$  dominates in both the numerator and denominator, causing  $a$  to tend towards 1. Note that this maximum value of  $a$  is very close to  $a = 0.91$  suggested by Wu and Pan (1997) from numerical simulations conducted on differently textured soils. Conversely, for large rings or coarse soils, the first term dominates in both the numerator and the denominator and  $a$  tends towards  $\frac{2-\beta}{3}$ , which equals 0.467 for  $\beta = 0.6$ . In a similar way, for a given soil, as  $r_d$  increases, the contribution of the lateral capillarity decreases and the flow is dominated by gravity resulting in a decreasing  $a$  value that again approaches  $\frac{2-\beta}{3} = 0.467$  (for  $\beta = 0.6$ ) as  $r_d \rightarrow \infty$ . Note that this minimum value of  $a$  is very close to  $a = 0.45$  suggested by Stewart and Abou Najm (2018a) based on analogy with 1D infiltration. Overall, this analysis shows that  $a$  cannot be considered a constant regardless of soil type and experimental conditions, but instead represents a scale parameter between transient and steady infiltration rates for a single ring three-dimensional infiltration process.

## Investigation of $\tau_{crit}$ with the approach by Haverkamp et al. (1994) and Lassabatere et al. (2006)

On the basis of the approximate expansions defined by Haverkamp et al. (1994), Lassabatere et al. (2006) defined the maximum time  $t_{max}$  involved in Eq.(7) as the time that separates the transient



from the steady states. These authors specifically evaluated  $t_{max}$  by differentiating Eq.(7), which showed that the transient infiltration rate,  $q_{tst}(t)$ , decreases from infinity to  $q_{tst,+\infty} = \frac{2-\beta}{3}\Delta K + K_i + \frac{\gamma S^2}{r_d\Delta\theta}$ , whereas the steady state infiltration rate,  $q_{sst}(t)$ , remains constant at  $q_{+\infty} = K_s + \frac{\gamma S^2}{r_d\Delta\theta}$ . Since  $q_{tst,+\infty} < q_{+\infty}$ , there is a time for which the transient infiltration rate  $q_{tst}(t)$  equals  $q_{+\infty}$ , which allows  $t_{max}$  to be defined as follows:

$$t_{max} = \frac{1}{4(1-B)^2} \left( \frac{S}{K_s} \right)^2 \quad (10)$$

in which  $(S/K_s)^2$  is the gravity time ( $t_{grav}$ ) defined by Philip (1969), and where:

$$B = \frac{2-\beta}{3} \frac{\Delta K}{K_s} + \frac{K_i}{K_s} \approx \frac{2-\beta}{3} \quad (11).$$

Note that the approximation  $B = \frac{2-\beta}{3}$  accounts for the fact that  $K_i \ll K_s$  when  $\theta_i \ll \theta_s$ . This remains the case for most initial water contents that fulfill the assumption of validity of Haverkamp's model, i.e.,  $\theta_i \leq 0.25 \theta_s$ .

The determination of  $t_{max}$  on the basis of infiltration rates is similar to the definition of  $\tau_{crit}$  by Stewart and Abou Najm (2018a,b). Here we simplify their expression by using the White and Sully (1987) equation for sorptivity and considering the case of a Beerkan test, i.e., a zero water pressure head at surface and a shallow depth of ring insertion ( $h_{source} = 0$ ;  $d = 0$ ). Under these conditions, Eq.(1c) can be written as:

$$\tau_{crit} = \frac{1}{4f^2(1-a)^2\Delta K} \left( \frac{S}{K_s} \right)^2 \approx \frac{1}{4f^2(1-a)^2} \left( \frac{S}{K_s} \right)^2 \quad (12).$$

Finally, comparing Eqs.(10) and (12) we arrive at the following relationship between  $\tau_{crit}$  and  $t_{max}$ :

$$\tau_{crit} = \frac{(1-B)^2}{f^2(1-a)^2} t_{max} \quad (13).$$

Thus, the two characteristic times ( $\tau_{crit}$  and  $t_{max}$ ) are related by a proportionality constant that depends on soil properties and initial conditions as well as ring radius.

## MATERIALS AND METHODS

Both analytically generated and field measured infiltration data were used in this investigation [dataset] (Iovino et al., 2021). The former data were used to exclude experimental errors while the latter ones were considered since the infiltration model is oriented towards field use.

### Analytically generated infiltration data

Infiltration data were analytically generated with the 3D implicit model of Haverkamp et al. (1994) to obtain estimates of  $\tau_{crit}$  and  $a$  for ideal soil conditions (error-free synthetic data). A total of 144

254 Beerkan infiltration runs were modeled for the six soils (sand, loamy sand, sandy loam, loam, silt  
 255 loam and silty clay loam), which were considered by Hinnell et al. (2009) to cover a wide range of  
 256 hydraulic responses. The parameters by Carsel and Parrish (1988) were used to describe the water  
 257 retention curve and the hydraulic conductivity function of these soils according to the van  
 258 Genuchten-Mualem model (van Genuchten, 1980). The infiltration parameters were set at the  
 259 recommended values of  $\beta = 0.6$  and  $\gamma = 0.75$  (Haverkamp et al., 1994; Smettem et al., 1994). The  
 260 question of this choice of  $\beta$  and  $\gamma$  was investigated by Lassabatere et al. (2009), who compared the  
 261 implicit infiltration model of Haverkamp et al. (1994) with a numerical solution of Richards'  
 262 equation. They showed that a specific calibration of infiltration parameters can improve prediction  
 263 of cumulative infiltration. However, using the default values of infiltration parameters did not  
 264 compromise estimation of  $S$  and  $K_s$  obtained by inverting the implicit model (Latorre et al., 2018).  
 265 The initial water content was calculated based on the degree of saturation,  $S_e$ , where  $S_e = (\theta_i - \theta_r)/(\theta_s$   
 266  $- \theta_r)$  and  $\theta_i$ ,  $\theta_r$  and  $\theta_s$  represent the respective initial, residual and saturated volumetric soil water  
 267 contents. The model was run with  $S_e$  values of 0.1, 0.2, 0.3, 0.4, 0.5, 0.6, 0.7 and 0.8, with three ring  
 268 radii of  $r_d = 40, 75$  and  $150$  mm simulated for each  $S_e$  value. We note that previous work has  
 269 recommended that values of  $\theta_i/\theta_s$  should not exceed 0.25 for Eqs.(7) and (8) to remain valid  
 270 (Lassabatere et al., 2006, Lassabatere et al., 2009); however, wetter conditions often occur in  
 271 practice (Di Prima et al., 2016) and, therefore, it makes sense to test the analytical models under  
 272 these conditions. The duration of each run was fixed at  $3 \times t_{max}$ , with  $t_{max}$  calculated according to  
 273 Eq.(10), to obtain data for both the transient and the steady-state phases of the infiltration process.  
 274 Each simulation consisted of 50  $I(t)$  data pairs. Other details on the simulation procedure can be  
 275 found in Bagarello et al. (2017).  
 276 In this study, we used an iterative procedure to find the optimal set of infiltration coefficients  $c_1$ ,  $c_2$ ,  
 277  $c_3$ ,  $c_4$  and their associated  $\tau_{crit}$  value. This method consisted of fixing a tentative time,  $t_j$ , to separate  
 278 transient ( $t < t_j$ ) and steady-state ( $t \geq t_j$ ) conditions. Then,  $c_1$ ,  $c_2$  and  $c_4$  were estimated by fitting  
 279 Eqs.(4a) and (4b) to the data with  $c_3$  defined by Eq.(5). The corresponding  $\tau_{crit,j}$  value was then  
 280 calculated by Eq.(4c) and the absolute difference between  $t_j$  and  $\tau_{crit,j}$  is determined. The procedure  
 281 was repeated for a range of  $t_j$  values. The optimal parameter values were then identified as those  
 282 yielding the minimum value, i.e.,  $\min(|t_j - \tau_{crit,j}|)$ .  
 283 For each infiltration run, 40 iterations were conducted with  $t_j$  time starting from the fifth  $I(t)$  data  
 284 point and ending at the 45<sup>th</sup>  $I(t)$  data point. This choice allowed a minimum infiltration dataset of  
 285 five points to fit either the transient or the steady-state stage of the infiltration process. For a  
 286 tentative time,  $t_i$ , linear regression was applied to fit Eq.(4b) to steady-state infiltration data ( $t \geq t_j$ ).

The fitting of Eq.(4a) to the transient infiltration data ( $t < t_j$ ) was conducted with a non-linear least squares optimization technique that minimized the squared differences between measured and predicted cumulative infiltration (Vandervaere et al., 2000; Lassabatere et al., 2006). Such approach was hereinafter indicated as criterion IT-CI (transient cumulative infiltration data fitted by non-linear least squares technique). To explore the influence of the fitting technique on the estimation of coefficients  $c_1$  and  $c_2$ , a second optimization procedure was conducted using the cumulative linearization technique proposed by Smiles and Knight (1976) (criterion IT-CL). The main characteristics of the different criteria for applying the SA model to the infiltration data are summarized in **Table 1**.

The maximum error,  $E_{max}$ , normalized by the final cumulative infiltration, was determined using:

$$E_{max} = \max \frac{|I_{opt} - I|}{I_f} \quad (14)$$

where  $I_{opt}$  is the cumulative infiltration estimated by Eqs.(4a) and (4b) with the optimal set of coefficients,  $I$  is the corresponding analytically calculated value, and  $I_f$  is cumulative infiltration at the end of simulation (i.e.,  $t = 3 \times t_{max}$ ). Using the optimal set of coefficients, the  $a$  constant was calculated by Eq.(6). The transition time,  $\tau_{crit}$ , estimated by the iterative procedure was compared to  $t_{max}$  to evaluate proportionality between the two characteristic times.

We also conducted a sensitivity analysis of  $a$  values estimated by the iterative criterion by fixing  $\tau_{crit}$  at  $t_{max}$  (i.e., one third of the total duration of the experiment, since modelling was performed for time up to  $3 t_{max}$ ). Eq.(4a) was fitted to the transient ( $t < t_{max}$ ) data by a non-linear least squares optimization technique and Eq.(4b) was fitted to steady-state ( $t \geq t_{max}$ ) portions of the run by linear regression. The scaling parameter  $a$  was then calculated from Eq.(6).

### Field experiment

Two Sicilian soils were chosen for this investigation. A loam soil (AR site) was located at the Department of Agricultural, Food and Forest Sciences of the Palermo University (Italy). A silty-clay soil (RO site) was located near Roccamena, approximately 70 km south of Palermo. The AR soil supported a citrus orchard under no tillage. The RO soil supported a fruit orchard under no tillage. Soil at the AR site was sampled on five different dates (November 2017, April, May and September 2018, April 2019) to encompass a range of environmental conditions. Soil was sampled only once at RO sites (June 2019). The same experimental protocol was applied for each of the overall six sampling campaigns.

For each sampling campaign, 10 infiltration runs were carried out at randomly selected locations within a bare area of approximately 150 m<sup>2</sup>. At each infiltration site, the sampled soil surface was gently leveled and smoothed by manual implements. Small diameter (0.08 m) rings were inserted

on the soil surface to a depth of 0.01 m following the Beerkan infiltration procedure (Lassabatere et al., 2006). Ring insertion was conducted manually by gently using, if necessary, a rubber hammer, while ensuring that the upper rim of the ring remained horizontal during insertion. Then, 30 water volumes, each of 57 mL, were successively poured onto the confined infiltration surface. A relatively large cumulative infiltration height (approximately 0.34 m of water) was used to attain quasi-steady state conditions. For each water volume, the infiltration time was measured from water application to disappearance of all water, when the subsequent water volume was poured on the infiltration surface. Water was applied at a small distance from the infiltration surface, i.e., approximately at a height,  $h_w$ , of 0.03 m, with the practitioner's fingers used to dissipate the kinetic energy of the falling water and thereby minimize soil disturbance due to water application. After the infiltration test, two undisturbed soil cores (0.05 m in height by 0.05 m in diameter) were collected nearby at 0 to 0.05 m and 0.05 to 0.10 m depths. These cores were used to determine the dry soil bulk density,  $\rho_b$ , and the initial soil water content,  $\theta_i$ . The data were averaged over the two depths and paired with the corresponding infiltration run (**Table 2**).

The iterative criterion set up for analytical data (IT-CI) was also applied to field data to simultaneously estimate the infiltration coefficients ( $c_1$ ,  $c_2$ ,  $c_3$ , and  $c_4$ , with  $c_3$  constrained by Eq.5), the transition time, and the related  $a$  value.

In addition to the above procedure, we also tested a more practical approach to fit the SA model to the infiltration data. We first split the cumulative infiltration for each run into transient versus steady state, specifically by estimating the transition time,  $\tau_{crit}$ , according to the empirical criterion proposed by Di Prima et al. (2019). We presumed that steady-state conditions were reached before the end of the run, where the total run corresponded to  $N_{tot}$  data points, and then carried out a linear regression analysis on the last  $n$  data pairs  $(t_i, I_i)$   $i \in \{N_{tot}-n+1, \dots, N_{tot}\}$ . Then, we computed the relative error between the regression line  $I_{reg,n}(t_i)$  and the observed cumulative infiltration  $I(t_i)$ :

$$\hat{E}(n) = \left| \frac{I(t_{N_{tot}-n+1}) - I_{reg,n}(t_{N_{tot}-n+1})}{I(t_{N_{tot}-n+1})} \right| \quad (15)$$

A minimum of three points ( $n = 3$ ) was considered for steady state. In this case,  $\hat{E}(n = 3)$  is usually small and results from measurement uncertainty. When more points are selected, a part of transient state is included that diverts from the steady-state straight line. In particular, the largest error is obtained when all the points ( $n = N_{tot}$ ) are considered for estimating the regression line. Therefore,  $\hat{E}(n)$  defines an increasing function. We selected the first value of  $n$  for which  $\hat{E}(n) \geq E$ , where  $E$  is a given threshold that in this study was fixed at 2% (Bagarello et al., 1999). The transition time was then defined as the corresponding time,  $\tau_{crit} = t_{N_{tot}-n+1}$ . Transient infiltration conditions

were assumed to occur for  $0 < t < \tau_{crit}$  (i.e., when  $\hat{E} \geq 2\%$ ). Steady-state conditions were assumed to exist for  $t \geq \tau_{crit}$  (i.e., when  $\hat{E} < 2\%$ ).

Once the cumulative infiltration was split into transient and steady states, the SA model was fitted to each part of the infiltration process. The cumulative infiltration (CI) fitting method (Vandervaere et al., 2000), that corresponds to non-linear least squares optimization technique, was applied by fitting Eq.(4a) to the transient stage of infiltration. The quality of the fit was evaluated by calculating the relative error,  $Er$  (%), as suggested by Lassabatere et al., 2006:

$$Er = 100 \sqrt{\frac{\sum_{i=1}^k (I_i^{\exp} - I_i)^2}{\sum_{i=1}^k (I_i^{\exp})^2}} \quad (16)$$

where  $I_i^{\exp}$  and  $I_i$  are the experimental and modeled cumulative infiltration for the period of  $0 < t < \tau_{crit}$ . Next, linear regression analysis of the  $I(t)$  data at steady state ( $t \geq \tau_{crit}$ ) was used to estimate the  $c_3$  and  $c_4$  coefficients of Eq.(4b). Finally,  $a$  was calculated by Eq.(6). This iterative procedure is denoted as criterion EV-CI (V = variable number of data points). We also considered the simpler case of a regression line defined by the last three points of the cumulative infiltration. The corresponding method is denoted E3-CI. For these procedures (i.e., EV-VI and E3-CI), we considered a run to be successful when all coefficients ( $c_1$ ,  $c_2$ ,  $c_3$  and  $c_4$ ) were positive since, according to Eq.(1), they cannot be negative or null. With the aim to give the model the maximum flexibility in fitting experimental data, the coefficients were left unconstrained, meaning that we did not constrain  $c_3$  using Eq.(5) in this portion of the analysis (see Table 1).

We also attempted to verify the possible existence of a link between the shape of the experimentally determined infiltration curve and the results of the  $a$  calculations. At this aim, we fitted the empirical Horton (1940) infiltration model to the data:

$$I = i_f t + \frac{i_0 - i_f}{k} (1 - e^{-kt}) \quad (17)$$

where  $i_0$  ( $L T^{-1}$ ) is the initial infiltration rate ( $t = 0$ ),  $i_f$  ( $L T^{-1}$ ) is the final infiltration rate and the constant  $k$  ( $T^{-1}$ ) determines the rate at which  $i_0$  approaches  $i_f$ . This model was chosen instead of other possible alternatives (e.g. numerical solution of Richards equation) as we target simpler analytical solutions and practical approaches to solving the infiltration problem. Indeed, it describes in some detail the complete infiltration curve using only three parameters, and it was found to give a good representation of the experimentally determined  $I(t)$  relationships in other investigations (Shukla et al., 2003).

## RESULTS AND DISCUSSION

### Analytically generated infiltration data

#### Critical time

As an example, **Fig. 1a** shows the analysis conducted by criterion IT-CI for one of the 144 synthetic infiltration runs. Here, the simulation time  $t_j$  (corresponding to data points  $5 \leq j \leq 45$ ) was used as the initial assumed value to differentiate between transient and steady-state data. The corresponding  $\tau_{crit,j}$  values were then calculated based on the fitted  $c_1$ ,  $c_2$ ,  $c_3$ , and  $c_4$  coefficients (expressed as a fraction of the optimal value of each coefficient in **Fig. 1b**). The absolute differences between  $t_j$  and  $\tau_{crit,j}$  shows a clear minimum at  $j = 24$ . This minimum is close to, but not quite, zero due to the discretization of the  $I(t)$  data. All tested experiments showed similar distinct minimum values for  $|t_j - \tau_{crit,j}|$ . Cumulative infiltration for this experiment is shown in **Fig. 1c** with the fitted models Eq.(4a) and Eq.(4b) corresponding to the optimal set of coefficients. The maximum error for this case was  $E_{max} = 0.0031$ , whereas for the entire dataset ( $N = 144$ )  $E_{max}$  varied between 0.0015 and 0.0042, with a mean value of 0.0029 (**Table 3**).

The critical time estimated by the criterion IT-CI varied by more than three orders of magnitude: the ratio between the highest and lowest  $\tau_{crit}$  values was 2650. The IT-CI algorithm resulted in  $\tau_{crit}$  values that were systematically higher than the values estimated using the IT-CL algorithm (**Table 3**), with a constant factor of 1.096 between the two. This result confirmed that fitting the transient stage of the infiltration process is a challenging task even with analytical (i.e., error-free) data. As a matter of fact, estimates of  $c_1$  with the two techniques differed by a constant factor of 1.022 and the estimates of  $c_2$  differed by a mean factor of 1.013 (min = 1.006, max = 1.028). In other words, applying the cumulative linearization technique (IT-CL), instead of the non-linear least squares technique (IT-CI), resulted in a relative overestimation of coefficient  $c_1$  and a relative underestimation of  $c_2$  due to the inter-compensation between the two coefficients (Vandervaere et al., 2000). In turn, such differences yielded a different selection of the transient or steady-state data and, consequently, different estimates for both the  $\tau_{crit}$  and  $a$  parameters. Nonetheless, the  $a$  values estimated by the two transient fitting techniques were highly correlated ( $R^2 > 0.999$ ) and the criterion IT-CI overestimated  $a$  by a mean factor of 1.017 compared to criterion IT-CL (**Table 3**). Moreover, for each combination of soil, ring diameter and initial water saturation, the factor of discrepancy between the estimated  $a$  values using the two fitting techniques was in the range of 1.008-1.029. Thus, the influence of the fitting technique on the prediction of  $a$  can be considered small and probably negligible in practice. For the subsequent analyses, only the results obtained by



the non-linear least squares technique (criterion IT-CI) were considered, as that approach was also consistent with the criterion applied for the field data.

The analytical data confirmed the proportionality between  $\tau_{crit}$  and  $t_{max}$ , that was theoretically expressed by Eq.(13), for all types of soils. In particular, for the analytical infiltration experiments performed in this study, the ratio  $\tau_{crit}/t_{max}$  was constant and equal to 1.495, regardless of the combination of soil, ring diameter and initial water saturation (**Fig. 2a**). It is worth noting that this ratio was obtained for  $\beta = 0.6$ , and may be subject to change as  $\beta$  varies. Also, as stated in the methods section, we tested the sensitivity of  $a$  estimates by fixing  $\tau_{crit}$  at  $t_{max}$ . That comparison showed that the two sets of estimated  $a$  values were highly correlated but that those values obtained by the iterative criterion (**Fig. 2b**) were larger by a mean factor of 1.02 than those obtained under the assumption of equal characteristic times ( $0.71 \leq a \leq 0.90$  with criterion IT-CI and  $0.68 \leq a \leq 0.89$  with  $\tau_{crit} = t_{max}$ ). This analysis of sensitivity confirmed that  $t_{max}$  does not represent an accurate estimate of the transition time of the Stewart and Abou Najm (2018a) model. Nonetheless, differences in the estimation of  $\tau_{crit}$  up to a factor of 1.5 yielded estimations of  $a$  that were practically coincident (i.e., differing from one another by at most a factor of 1.04).

#### *Coefficients of the infiltration model*

**Fig. 3** summarizes the optimal values of the infiltration model coefficients,  $c_1$ ,  $c_2$ ,  $c_3$ ,  $c_4$ , obtained for each soil, ring diameter and initial soil water saturation. Similarities can be noted between  $c_1$  and  $c_3$ , and again between  $c_2$  and  $c_4$ . Further,  $c_2$  and  $c_4$  are nearly constant regardless of  $S_e$ , indicating the importance of  $K_s$  relative to the macroscopic capillary length within the factor  $f$  (Eq.2), since only the latter will decrease with  $S_e$ . The results also show that capillarity is relatively more important in small rings (e.g.,  $r_d = 40$  mm) compared to large rings (e.g.,  $r_d = 150$  mm) as a consequence of lateral sorption representing more of the total flow when the ring perimeter is relatively large compared to the ring area. This process means that the values of  $c_2$  and  $c_4$  are higher and the reductions with increasing  $S_e$  more evident in the smaller rings compared to the larger ones.

At the same time, the  $c_1$  coefficient represents soil sorptivity in these infiltration models, so the reported curves appear physically plausible since they decrease as the initial saturation degree  $S_e$  increases. Indeed, we expect sorptivity, i.e. capillarity driven infiltration, to be at its maximum for initially dry soils. Moreover, early time infiltration is governed by vertical capillary-driven flow and does not depend on the 3D flow term; therefore, ring size has no effect on the estimates of the  $c_1$  coefficient. It is worth noting that, with the analytically generated cumulative infiltration curves, the coefficient  $c_3$  is also independent of ring size. This result is a consequence of the assumed



continuity of the transient and steady-state infiltration curves at the transition time, which is specified by Eq.(5).

The meaningful trends of the estimated coefficients (**Fig. 3**), and the consistency with the constraints of the Stewart and Abou Najm (2018a) model, prove that the iteration criterion used for analyzing the synthetic infiltration data was effective in estimating the transition time  $\tau_{crit}$  and the associated set of coefficients  $c_1, c_2, c_3, c_4$ .

#### *a* parameter

The results of the iterative criterion were thus used to test the effects of initial water content and ring radius on the  $a$  constant of SA model (**Fig. 3, last row**). The  $a$  values calculated by Eq.(6), using the infiltration coefficients estimated by the iterative approach IT-CI, varied between 0.706 and 0.904, with a mean of  $a = 0.807$  (**Table 3**). Therefore, the iterative procedure yielded  $a$  parameter values that were, on average, closer to the value suggested by Wu and Pan (1997) than the recommendations of Stewart and Abou Najm (2018a). Soil texture affected the  $a$  constant, with the sandy and sandy loam soils having the lowest  $a$  values and the silt loam and silty clay loam soils yielding the highest  $a$  values. The  $a$  parameter decreased as the ring diameter increased and was more influenced by ring size than initial water content.

It must be noted that the synthetic infiltration data were obtained by the implicit model developed by Haverkamp et al. (1994) and that those authors suggested using their model only when the initial water content is lower than 0.25 of the saturated water content. Despite this potential limitation, our results show that the value of  $a$  remains strictly constant for  $S_e < 0.5$ , and its value only slightly varied when the initial degree of saturation was in the range  $0.5 \leq S_e \leq 0.8$ . Therefore, the simplification presented in Eq.(9), which suggests that  $a$  depends only on ring size and soil properties such as  $\lambda_{max}$  and  $K_s$ , appears to be valid for a fairly wide range of initial water contents.

#### **Field experiments**

The average duration of the 60 infiltration tests was of 0.78 h ( $CV = 105.6\%$ ). Application of the most rigorous criterion, IT-CI, only succeeded in 25 out of 60 infiltration tests (42% success rate). In most cases, failure was due to the lack of a well-defined minimum for the  $|t_j - t_{crit,j}|$  function. The successful runs had a mean duration of 0.77 h and a mean  $\tau_{crit}$  of 0.57 h. The constrained fitting of the infiltration coefficients resulted, in some cases, in low or negative values of  $c_3$  that is the intercept of the regression line fitting the steady-state stage of the infiltration curve (**Table 4**). The 25 experiments that were successfully treated with the IT-CI criterion yielded a mean  $a$  value of

0.883 ( $CV = 26.1\%$ ). Calculated  $a$  values were implausible in 5 out of 25 successful runs (i.e.,  $a > 1$ ). Excluding these values from the analysis yielded a mean value  $a = 0.783$  ( $CV = 14.5\%$ ,  $N = 20$ ) (Table 4).

As explained in the methods section, we also tested two empirical criteria as simpler methods for estimating the transition time: E3-CI and EV-CI. An example of these two fitting procedures is shown in Fig. 4. When we used the E3-CI criterion, 44 out of 60 infiltration tests were successfully fitted (i.e., positive infiltration coefficients), representing a success rate of 73%. The successful runs had a mean duration of 0.96 h and a mean  $\tau_{crit}$  of 0.58 h, while the unsuccessful runs had a mean duration of 0.31 h and a mean  $\tau_{crit}$  of 0.19 h. Application of the more flexible criterion for assessing the steady-state (i.e., criterion EV-CI) resulted in a similar success rate, as estimation succeeded in 43 out of 60 cases (72% success rate). The number of cumulative infiltration data defining the steady-state infiltration stage ranged from a minimum of 9 to a maximum of 15. The successful runs had a mean duration of 0.98 h and a mean  $\tau_{crit}$  of 0.44 h, while the unsuccessful runs had a mean duration of 0.30 h and a mean  $\tau_{crit}$  of 0.16 h.

Reasons of failure included obtaining  $c_1 = 0$  (9 cases for E3-CI and 10 cases for EV-CI),  $c_1 = 0$  and  $c_3 < 0$  (4 cases with both E3-CI and EV-CI), and  $c_2 = 0$  (3 cases with both E3-CI and EV-CI). We note that the iterative criterion (IT-CI) also failed for all of the aforementioned infiltration runs, leading to the conclusion that estimating the transition time can identify tests that do not follow theory, regardless of the applied criterion. The  $c_2 = 0$  results were associated with high  $c_1$  values ( $> 440 \text{ mm/h}^{0.5}$ ), i.e., high apparent soil sorptivity (Fig. 5, points located on the y-axis). On the other hand,  $c_1 = 0$  results were associated with high  $c_2$  values ( $> 600 \text{ mm/h}$ ), i.e., high apparent saturated conductivity (Fig. 5, points located on the x-axis). These two extreme scenarios are typical of two opposite types of soils, i.e., fine soils prone to capillarity-driven flow on one hand, and coarse soils prone to gravity-driven flow on the other. Experimental runs thus confirmed that possible inter-compensation between the coefficients  $c_1$  and  $c_2$  may complicate fitting of the transient infiltration relationship. Fig. 6 shows an example of the cumulative infiltration curve for each reason of failure. In short, runs failed when i)  $I$  was nearly linear with  $t$  (lack or very short duration of an initial transient phase, Fig. 6a) (Angulo-Jaramillo et al., 2019), ii) the infiltration rates increased with time, as expected in water repellent soil conditions (Fig. 6b) (Beatty and Smith, 2013; Ebel and Moody, 2013), and iii) concavity was or appeared to be particularly pronounced, as for sealing soils (Di Prima et al., 2018) (Fig. 6c).

Criterion E3-CI, being based on the last three cumulative infiltration data, generally yielded higher  $\tau_{crit}$  values compared to criterion EV-CI, which estimated the steady-state infiltration from a larger dataset (Fig. 4). According to criterion E3-CI, the mean  $\tau_{crit}$  value was equal to 0.47 h ( $CV =$

100.3%). When criterion EV-CI was used to estimate the steady-state stage of the infiltration process, the mean  $\tau_{crit}$  was 0.36 h ( $CV = 93.8\%$ ), i.e., 18% lower than the mean critical time estimated by criterion E3-CI. In both cases, the critical time increased with the duration of the run (Fig. 7).

Despite the different estimates of the transition time, the two empirical criteria (E3-CI and EV-CI) were almost equivalent in estimating the coefficients  $c_1$ ,  $c_2$ ,  $c_3$  and  $c_4$  of Eq.(4) as showed by the high values of the correlation coefficient ( $0.936 \leq r^2 \leq 0.997$ ). In particular, selecting a longer steady-state interval, as per criterion EV-CI, resulted in the estimates for coefficient  $c_3$  that were lower than those of the E3-CI method by a mean factor of 1.18 (Table 4). Conversely, coefficient  $c_4$  attained using EV-CI was larger by a mean factor of 1.07 than those of E3-CI. The field data thus confirmed the results obtained with analytical data, specifically that differences when identifying the relative duration of transient versus steady-state infiltration stages had minor influence on estimated infiltration coefficients.

We did not impose a constraint for coefficient  $c_3$  for either empirical criteria (i.e., E3-CI and EV-CI), because in both cases the transition time was assumed a-priori and independently from the fitted infiltration coefficients. This simplification implies that the fitted cumulative infiltration curve may be discontinuous for  $t = \tau_{crit}$ . As a matter of fact, for the 43 successful runs with both criteria, the estimates of  $I$  calculated for  $t = \tau_{crit}$  with the transient (Eq.4a) and the steady-state (Eq.4b) models differed by a percentage ranging from -6.6% to 2.9%. The fitting algorithms therefore identify parameter values that can vary from the theoretical constraints placed by the SA model. Nonetheless, these results still show that the tested empirical algorithms are sufficiently reliable to interpret field measurements, with the specific advantage of being simpler to apply compared to iterative criterion.

At the same time, it is likely that the unconstrained  $c_3$  values had little or no influence on the calculations of the  $a$  constant, as that term was estimated only with the  $c_2$  and  $c_4$  coefficients. The valid infiltration runs yielded  $a$  values varying from 0.239 to 1.690. The null hypothesis that the positive  $a$  values were normally distributed was not rejected (Lilliefors 1967 test;  $\alpha = 0.05$ ); consequently, the  $a$  values were summarized by the arithmetic mean and the associated  $CV$  (Table 4).

For the 44 runs that yielded positive  $a$  results with criterion E3-CI, the relative error of the transient infiltration model,  $Er$ , was  $\leq 6.1\%$  (mean = 2.2%). In addition,  $Er$  was less than 3.5% in the 86.4% of the cases, denoting a good fit of the model to the data considering a threshold of 5% as suggested by Lassabatere et al. (2006). For the 43 runs that yielded positive  $a$  results with criterion EV-CI,  $Er$  was  $\leq 3.8\%$  (mean = 1.7%), thus denoting a better fitting of the model as compared to criterion E3-

CI. Nonetheless, the  $a$  values obtained by the two approaches (E3-CI and EV-CI) differed by a nearly negligible mean factor of 1.10 (**Table 4**) and were significantly correlated ( $R^2 = 0.997$ ). However, a rather high percentage of calculated  $a$  values were implausible, as 20 out of 44 individual values were  $> 1$  with criterion E3-CI (i.e., 45% of tests). An even larger percentage of physically implausible values (i.e.,  $a > 1$ ) were obtained by criterion EV-CI (55% of tests). Excluding values of  $a > 1$  from the analysis, the mean  $a$  parameter values were similar between criteria:  $a = 0.735$  for E3-CI and  $a = 0.737$  for EV-CI. The  $CV$  of the individual estimates of  $a < 1$  (27.9%-32.3%) was much lower than the  $CV$ s of  $c_2$  and  $c_4$  (**Table 4**).

Altogether, the results of this field investigation were consistent with the analysis of the analytically generated infiltration data, since in both cases  $a$  was intermediate between the values suggested by Stewart and Abou Najm (2018a), i.e.,  $a = 0.45$ , and Wu and Pan (1997), i.e.,  $a = 0.91$ . However, the field experiments only led to successful  $a$  estimates in a limited number of cases. Specifically, 20 out of 60 tests (33%) were successful and had physically plausible  $a$  values when using IT-CI, 20 out of 60 tests were successful and plausible for EV-CI (33%) and 24 out of 60 tests were successful and plausible for E3-CI (40%). Implausible estimates of  $a$  could indicate infiltration tests that violates the model assumptions (i.e., homogeneous soil with uniform initial water content) or unsatisfactory description of the steady-state stage with the empirical criterion. In these cases, a practical recommendation could be to fix  $a$  at a value close to the maximum theoretical value ( $a = 1$ ) and proceed with a constrained estimation of the infiltration coefficients linear with time.

The Horton model was successfully fitted to the data for 52 out of the 60 infiltration experiments, and all failures occurred at the AR site. The  $Er$  values varied from 0.41 to 4.5% and were lowest at the AR site and highest at the RO site (**Table 5**). For the 44 infiltration runs yielding an estimate of the  $a$  constant by the criterion E3-CI, a scattered but rather clear relationship was detected between  $a$  and  $k/i_f$  ( $R^2 = 0.659$ ), representing a normalized  $k$  constant (**Fig. 8**). For these runs, the  $k/i_f$  ratio varied between 0.011 and 0.067  $\text{mm}^{-1}$ . For the 16 cases in which estimation of  $a$  failed, the Horton model was not applicable (eight runs) or  $k/i_f$  was either greater than 0.067  $\text{mm}^{-1}$  (4 runs) or smaller than 0.011  $\text{mm}^{-1}$  (three runs). In a single case, an estimate of  $a$  was not obtained, even though  $k/i_f$  equaled 0.025  $\text{mm}^{-1}$  (and therefore was in the range 0.011-0.067  $\text{mm}^{-1}$ ). Therefore, the rate at which the initial infiltration rate approached the final infiltration rate, expressed by normalized  $k$  constant, explained both variability of  $a$  and the success or the failure of the experiment. According to the fitted relationship of **Fig. 8**, obtaining  $a < 1$  requires a normalized  $k$  constant of more than 0.02  $\text{mm}^{-1}$ .

## CONCLUSIONS

Applying the comprehensive infiltration model by Stewart and Abou Najm (SA model) requires estimating the transition time from transient to steady-state flow conditions,  $\tau_{crit}$ , and choosing a value for the so-called  $a$  constant. In previous tests of the SA model,  $\tau_{crit}$  was estimated by an empirical criterion based on the premise that the last three infiltration data points describe steady-state conditions, yet that approach had not been rigorously analyzed. Further, the SA model included a recommendation to fix  $a$  at a constant value of 0.45, half of the value ( $a = 0.91$ ) that had been proposed in earlier studies. These differences in assumed values for  $a$  can affect the model performance, particularly when it is used to estimate soil hydraulic properties from infiltration tests. Given these uncertainties, this investigation introduced a novel, iterative method for estimating  $\tau_{crit}$  that includes the constraint that the same cumulative infiltration has to be obtained at the time  $t = \tau_{crit}$  with the transient and steady-state explicit expressions of the model. The new estimating criterion of  $\tau_{crit}$  is physically more robust than the existing estimating criterion since it does not require any a-priori assumptions about the number of data points associated with steady-state conditions. Instead, the new method was shown to fail if steady-state was not reached by the end of the infiltration run, meaning that the method is a valid and useful test of whether infiltration data can accurately be partitioned into transient and steady-state phases. Our tested algorithms all generated slightly different estimates for transition times for the same infiltration data, thus revealing some minor uncertainty associated with these methods. Nonetheless, the differences were for the most part minor, even when using relatively simple fitting algorithms, suggesting that empirical fitting methods are suitable in many instances.

This investigation also demonstrated that the  $a$  term of the SA model is not a constant and can plausibly vary over the  $0.47 < a < 1$  range. The  $a$  parameter tends to be larger when small water sources are used and for finer soils. Our analysis, which relied on comparing two parameters that were generated from the transient and steady-state infiltration phases, also determined some  $a$  values  $> 1$ . These results are physically implausible, and suggest that in those runs the infiltration phases may not have been accurately demarcated. In such instances, practitioners may consider fixing  $a$  at a high but theoretically plausible value (e.g.,  $a = 0.91$  or  $0.95$ ) and then adjusting the other model parameters as necessary. At the same time, this investigation demonstrated that  $a$  does not depend appreciably on the applied method to obtain  $\tau_{crit}$ . In other words, some uncertainty in the estimate of  $\tau_{crit}$  does not have a relevant impact on estimation of  $a$ . These findings together expand the applicability of the SA model by showing that  $a$  does not need to be fixed a-priori.

The methods for obtaining  $\tau_{crit}$  and  $a$  developed here reveal valuable linkages between theory and practice. Specifically, infiltration tests for which the  $\tau_{crit}$  estimating method fails or the fitted  $a$



parameter exceeds the range of the admissible values can indicate non-ideal infiltration conditions. In these instances, analytical solutions such as the SA model will likely not provide satisfactory descriptions of the processes at work (e.g., non-ideal behaviors related to water repellency or heterogenous flow). In contrast, infiltration runs that result in appropriately constrained  $\tau_{crit}$  and  $a$  values are likely to yield more accurate estimates for soil hydraulic properties, such as saturated soil hydraulic conductivity, when applying the SA model. Therefore, we suggest that this investigation has practical relevance, and that the findings presented here should form the basis of future work aimed at the theory and application of infiltration processes. In particular, carefully controlled experiments should be carried out on other soils to verify that the methods developed here can distinguish between successful and unsuccessful runs under various conditions.

## ACKNOWLEDGEMENTS

Authors wish to thank N. Auteri for conducting infiltration experiments at RO site.

## REFERENCES

- Angulo-Jaramillo, R., Bagarello, V., Di Prima, S., Gosset, A., Iovino, M., Lassabatere, L., 2019. Beerkan Estimation of Soil Transfer parameters (BEST) across soils and scales. *Journal of Hydrology* 576, 239-261.
- Angulo-Jaramillo, R., Bagarello, V., Iovino, M., Lassabatere, L., 2016. *Infiltration Measurements for Soil Hydraulic Characterization*. Springer International Publishing, Cham, pp. 383 pp.
- Bagarello, V., Di Prima, S., Iovino, M., 2017. Estimating saturated soil hydraulic conductivity by the near steady-state phase of a Beerkan infiltration test. *Geoderma* 303(Supplement C), 70-77.
- Bagarello, V., Iovino, M., D. Reynolds, W., 1999. Measuring Hydraulic Conductivity in a Cracking Clay Soil Using the Guelph Permeameter. *Transactions of the ASAE* 42(4), 957-964.
- Bagarello, V., Iovino, M., Lai, J., 2019. Accuracy of Saturated Soil Hydraulic Conductivity Estimated from Numerically Simulated Single-Ring Infiltrations. *Vadose Zone J* 18(1), 180122.
- Beatty, S.M., Smith, J.E., 2013. Dynamic soil water repellency and infiltration in post-wildfire soils. *Geoderma* 192, 160-172.
- Bouma, J., 1982. Measuring the Hydraulic Conductivity of Soil Horizons with Continuous Macropores. *Soil Sci Soc Am J* 46(2), 438-441.
- Carsel, R.F., Parrish, R.S., 1988. Developing Joint Probability-Distributions of Soil-Water Retention Characteristics. *Water Resour Res* 24(5), 755-769.
- Di Prima, S., Castellini, M., Abou Najm, M.R., Stewart, R.D., Angulo-Jaramillo, R., Winiarski, T., Lassabatere, L., 2019. Experimental assessment of a new comprehensive model for single ring infiltration data. *Journal of Hydrology* 573, 937-951.
- Di Prima, S., Lassabatere, L., Bagarello, V., Iovino, M., Angulo-Jaramillo, R., 2016. Testing a new automated single ring infiltrometer for Beerkan infiltration experiments. *Geoderma* 262(Supplement C), 20-34.
- Di Prima, S., Rodrigo-Comino, J., Novara, A., Iovino, M., Pirastru, M., Keesstra, S., Cerdà, A., 2018. Soil Physical Quality of Citrus Orchards Under Tillage, Herbicide, and Organic Managements. *Pedosphere* 28(3), 463-477.

- 662 Dohnal, M., Vogel, T., Dusek, J., Votrubova, J., Tesar, M., 2016. Interpretation of ponded  
663 infiltration data using numerical experiments. *Journal of Hydrology and Hydromechanics*  
664 64(3), 289-299.
- 665 Ebel, B.A., Moody, J.A., 2013. Rethinking infiltration in wildfire-affected soils. *Hydrological*  
666 *Processes* 27(10), 1510-1514.
- 667 Haverkamp, R., Ross, P.J., Smettem, K.R.J., Parlange, J.Y., 1994. 3-Dimensional Analysis of  
668 Infiltration from the Disc Infiltrometer .2. Physically-Based Infiltration Equation. *Water*  
669 *Resour Res* 30(11), 2931-2935.
- 670 Hinnell, A.C., Lazarovitch, N., Warrick, A.W., 2009. Explicit infiltration function for boreholes  
671 under constant head conditions. *Water Resour Res* 45.
- 672 Horton, R.E., 1940. An approach towards a physical interpretation of infiltration capacity. *Soil*  
673 *Science Society of America Proceedings*, 5:399-417.
- 674 Iovino, M., Abou Najm, M.R., Angulo-Jaramillo, R., Bagarello, V., Castellini, M., Concialdi, P., Di  
675 Prima, S., Lassabatere, L., Stewart, R.D., (2021), "Analytical and field data SA model",  
676 Mendeley Data, V1, doi: 10.17632/66yxdp2dtn.1
- 677 Lassabatere, L., Angulo-Jaramillo, R., Soria-Ugalde, J.M., Cuenca, R., Braud, I., Haverkamp, R.,  
678 2006. Beerkan estimation of soil transfer parameters through infiltration experiments -  
679 BEST. *Soil Sci Soc Am J* 70(2), 521-532.
- 680 Lassabatere, L., Angulo-Jaramillo, R., Soria-Ugalde, J.M., Šimůnek, J., Haverkamp, R., 2009.  
681 Numerical evaluation of a set of analytical infiltration equations. *Water Resources Research*  
682 45. <https://doi.org/10.1029/2009WR007941>
- 683 Latorre, B., Moret-Fernández, D., Lassabatere, L., Rahmati, M., López, M.V., Angulo-Jaramillo,  
684 R., Sorando, R., Comín, F., Jiménez, J.J., 2018. Influence of the  $\beta$  parameter of the  
685 Haverkamp model on the transient soil water infiltration curve. *J Hydrol* 564, 222-229.
- 686 Lazarovitch, N., Ben-Gal, A., Šimůnek, J., Shani, U., 2007. Uniqueness of Soil Hydraulic  
687 Parameters Determined by a Combined Wooding Inverse Approach. *Soil Sci Soc Am J*  
688 71(3), 860-865.
- 689 Philip, J.R., 1969. Theory of Infiltration. In: V.T. Chow (Ed.), *Advances in Hydrosience*. Elsevier,  
690 pp. 215-296.
- 691 Philip, J.R., 1990. Inverse solution for one-dimensional infiltration, and the ratio  $A/K1$ . *Water*  
692 *Resour Res* 26(9), 2023-2027.
- 693 Reynolds, W., Elrick, D., 2002. 3.4.1.1 Principles and parameter definitions. In: J.H. Dane, G.C.  
694 Topp (Eds.), *Methods of Soil Analysis, Part 4, Physical Methods*. Soil Sci. Soc. Am.,  
695 Madison, Wisconsin, USA, pp. 797-801.
- 696 Reynolds, W.D., Elrick, D.E., 1990. Ponded Infiltration from a Single Ring .1. Analysis of Steady  
697 Flow. *Soil Sci Soc Am J* 54(5), 1233-1241.
- 698 Russo, D., Bresler, E., Shani, U., Parker, J.C., 1991. Analyses of infiltration events in relation to  
699 determining soil hydraulic properties by inverse problem methodology. *Water Resour Res*  
700 27(6), 1361-1373.
- 701 Shukla, M.K., Lal, R., Unkefer, P., 2003. Experimental evaluation of infiltration models for  
702 different land use and soil management systems. *Soil Science*, 168(3): 178-191.
- 703 Šimůnek, J., Šejna, M., van Genuchten, M. Th., 2018. New features of the version 3 of the  
704 HYDRUS (2D/3D) computer software package. *Journal of Hydrology and Hydromechanics*,  
705 66(2), 133-142, doi: 10.1515/johh-2017-0050, 2018.
- 706 Smettem, K.R.J., Parlange, J.Y., Ross, P.J., Haverkamp, R., 1994. 3-Dimensional Analysis of  
707 Infiltration from the Disc Infiltrometer .1. A Capillary-Based Theory. *Water Resour Res*  
708 30(11), 2925-2929.
- 709 Smiles, D., Knight, J., 1976. A note on the use of the Philip infiltration equation. *Soil Research*  
710 14(1), 103-108.
- 711 Smith, R.E., Smettem, K.R.J., Broadbridge, P., Woolhiser, D.A., 2002. *Infiltration Theory for*  
712 *Hydrologic Applications*. American Geophysical Union, Water Resources Monograph.



- 713 Stewart, R.D., Abou Najm, M.R., 2018a. A Comprehensive Model for Single Ring Infiltration I:  
714 Initial Water Content and Soil Hydraulic Properties. *Soil Sci Soc Am J* 82(3), 548-557.
- 715 Stewart, R.D., Abou Najm, M.R., 2018b. A Comprehensive Model for Single Ring Infiltration II:  
716 Estimating Field-Saturated Hydraulic Conductivity. *Soil Sci Soc Am J* 82(3), 558-567.
- 717 van Genuchten, M.T., 1980. Closed-form equation for predicting the hydraulic conductivity of  
718 unsaturated soils. *Soil Sci Soc Am J* 44(5), 892-898.
- 719 Vandervaere, J.-P., Vauclin, M., Elrick, D.E., 2000. Transient Flow from Tension Infiltrometers I.  
720 The Two-Parameter Equation. *Soil Sci. Soc. Am. J.* 64(4), 1263-1272.
- 721 White, I., Sully, M.J., 1987. Macroscopic and microscopic capillary length and time scales from  
722 field infiltration. *Water Resour Res* 23(8), 1514-1522.
- 723 Wu, L., Pan, L., 1997. A Generalized Solution to Infiltration from Single-Ring Infiltrometers by  
724 Scaling. *Soil Sci. Soc. Am. J.* 61(5), 1318-1322.
- 725 Wu, L., Pan, L., Mitchell, J., Sanden, B., 1999. Measuring Saturated Hydraulic Conductivity using  
726 a Generalized Solution for Single-Ring Infiltrometers. *Soil Sci. Soc. Am. J.* 63(4), 788-792.

727

## FIGURE CAPTIONS

**Figure 1.** Example of application of iterative criterion IT-CI. In a) the values for  $t_j$ ,  $\tau_{crit,j}$ , and the absolute difference between the two,  $|t_j - \tau_{crit}|$ , are calculated for each data point  $j$  between 5 and 45. In b) the estimated parameters  $c_1$ ,  $c_2$ ,  $c_3$ , and  $c_4$  are expressed as fractions of the optimal value for each parameter,  $c_{i,opt}$ . In c) cumulative infiltration is modelled using Eq.(4) with the optimal set of parameters; the white dot shows the transition time.

**Figure 2.** Comparison between a) transition time  $\tau_{crit}$  and maximum time  $t_{max}$  for the analytically generated infiltration experiments; b) values of  $a$  constant estimated by the iterative criterion IT-CI and assuming  $\tau_{crit} = t_{max}$ .

**Figure 3.** Optimized coefficients  $c_1$ ,  $c_2$ ,  $c_3$  and  $c_4$  and  $a$  parameter as a function of initial degree of saturation,  $S_e$ , obtained for each soil and ring radius,  $r_d$ , by the iterative criterion IT-CI applied to analytically generated infiltration data.

**Figure 4.** Example of  $\tau_{crit}$  estimation by different approaches for identifying the steady-state stage of the infiltration process. Criterion E3-CI considers regression line fitting the last three data points. Criterion EV-CI considers regression line fitting the whole set of cumulative infiltration data for which  $\hat{E} \leq 2\%$  (Eq.(14)).

**Figure 5.** Scatter plot of the  $c_1$  vs.  $c_2$  coefficients estimated by criteria EV-CI (crosses) and E3-CI (circles). (sample size,  $N = 60$ )

**Figure 6.** Examples of unsuccessful runs: a)  $c_1 = 0$ ; b)  $c_1 = 0$  and  $c_3 < 0$ ; and c)  $c_2 = 0$ . Blue lines indicate the fitting of the transient model to the data and red lines indicate the adaption of the steady-state model to the data

**Figure 7.** Relationship between the total duration of the field run and the  $\tau_{crit}$  time estimated by criteria EV-CI (crosses) and E3-CI (circles). (sample size,  $N = 60$ )

**Figure 8.** Relationship between the estimated  $a$  parameter and the normalized  $k$  constant of the Horton infiltration model

762

763 **Table 1.** Characteristics of the different criteria considered in the study for applying the SA model  
 764 to analytical (A) or field (F) infiltration data.

Criterion	data	Transient time, $\tau_{crit}$ estimation	Fitting of transient infiltration data	Fitting of steady infiltration data	Parameter $a$ estimation
IT-CI	A, F	Iterative approach with coefficient $c_3$ constrained by Eq.5	Non-linear least squares technique	Linear regression	$a = c_2/c_4$
IT-CL	A	Iterative approach with coefficient $c_3$ constrained by Eq.5	Cumulative linearization technique (Smiles and Knight, 1976)		
EV-CI	F	Linear regression line with variable number of steady infiltration data ( $E = 2\%$ )	Non-linear least squares technique		
E3-CI	F	Linear regression line with 3 steady infiltration data ( $E = 2\%$ )	Non-linear least squares technique		

765

766

767

**Table 2.** Mean and coefficient of variation,  $CV$ , of the soil water content,  $\theta_i$ , and the dry soil bulk density,  $\rho_b$ , at the beginning of the infiltration run (sample size,  $N = 10$  for each summarized dataset)

Site	Date	$\theta_i$ (m <sup>3</sup> /m <sup>3</sup> )		$\rho_b$ (g/cm <sup>3</sup> )	
		mean	CV (%)	mean	CV (%)
AR	November 2017	0.215	6.5	0.966	6.0
	April 2018	0.199	15.3	0.957	11.1
	May 2018	0.137	12.0	0.979	7.9
	September 2018	0.103	11.8	1.037	6.9
	April 2019	0.158	21.8	1.064	5.5
RO	June 2019	0.184	16.1	0.998	7.1

$CV$  = coefficient of variation



**Table 4.** Statistics of infiltration coefficients and scale parameter  $a$  for the successful application of the iterative criterion IT-CI and the empirical criteria EV-CI and E3-CI. Statistics for plausible estimates of parameter  $a$  ( $a < 1$ ) are also reported.

	$c_1$ (mm h <sup>-0.5</sup> )	$c_2$ (mm h <sup>-1</sup> )	$c_3$ (mm)	$c_4$ (mm h <sup>-1</sup> )	$a$	$a < 1$
<b>Criterion IT-CI</b>						
N	25	25	25	25	25	20
min	56.0	7.0	-50.5	63.3	0.444	0.444
max	215.5	1432.2	185.3	1356.8	1.412	0.916
mean	131.3	633.8	2.0	555.2	0.883	0.783
CV(%)	36.2	58.4	3129.5	62.6	26.1	14.5
<b>Criterion EV-CI</b>						
N	43	43	43	43	43	19
min	3.5	19.7	30.3	63.9	0.270	0.270
max	361.3	2957.5	170.1	2556.0	1.690	0.954
mean	141.9	596.3	88.0	535.4	1.016	0.737
CV(%)	58.6	100.5	39.1	90.1	30.3	27.9
<b>Criterion E3-CI</b>						
N	44	44	44	44	44	24
min	38.2	19.4	33.9	60.9	0.239	0.239
max	463.3	2837.6	188.9	2487.4	1.364	0.976
mean	165.8	518.2	103.5	498.7	0.925	0.735
CV(%)	54.6	105.9	34.9	92.7	30.7	32.3

$N$  = sample size,  $Min$  = minimum value,  $Max$  = maximum value,  $CV$  = coefficient of variation

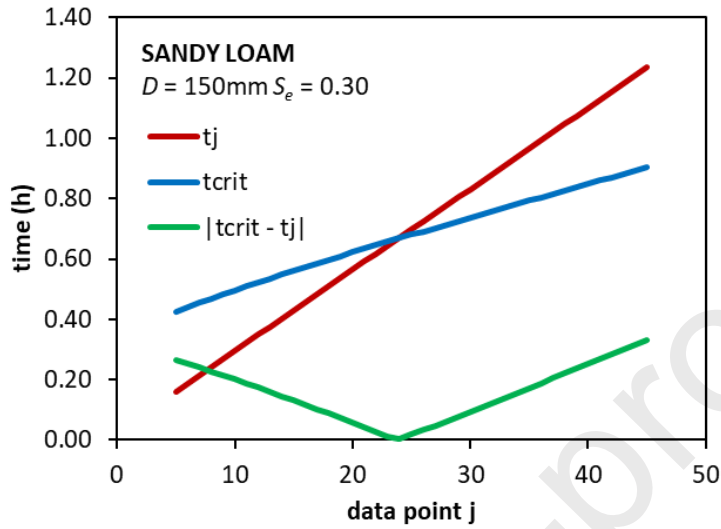
**Table 5.** Summary statistics of the initial infiltration rate,  $i_0$ , final infiltration rate,  $i_f$ , and the constant  $k$  of the Horton infiltration model for each sampled site

Site	Statistic	$i_0$ (mm h <sup>-1</sup> )	$i_f$ (mm h <sup>-1</sup> )	$k$ (h <sup>-1</sup> )	Er (%)
AR	N	42	42	42	42
	Min	200.1	9.53	0.093	0.41
	Max	4675.1	1370.2	67.1	4.10
	Mean	1470.0	320.7	8.05	1.29
	Median	1300.0	150.8	3.90	0.99
	CV (%)	62.4	89.6	152.0	61.1
RO	N	10	10	10	10
	Min	416.1	131.0	3.69	1.55
	Max	11243.0	716.1	70.1	4.46
	Mean	2734.2	328.6	19.9	2.89
	Median	890.3	247.5	6.73	2.45
	CV (%)	125.7	55.9	110.7	34.8

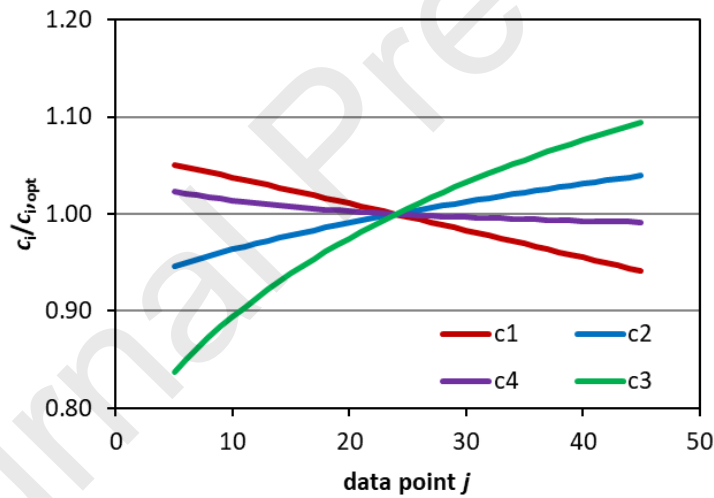
$N$  = sample size,  $Min$  = minimum value,  $Max$  = maximum value,  
 $CV$  = coefficient of variation



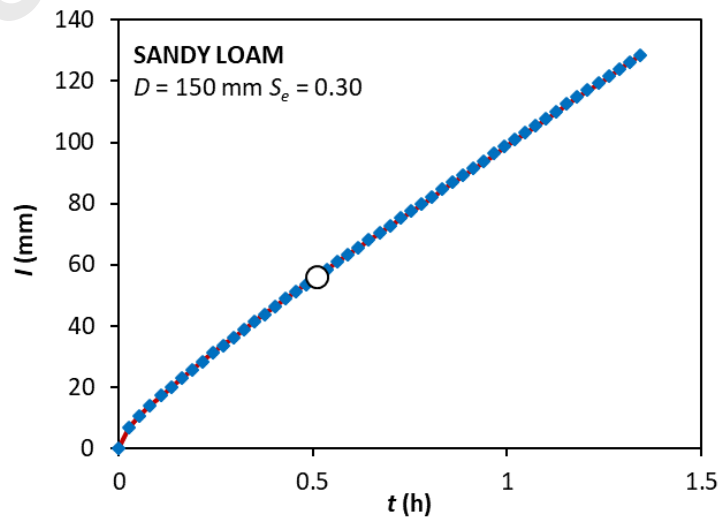
**Figure 1.** Example of application of iterative criterion IT-CI. In a) the values for  $t_j$ ,  $\tau_{crit,j}$ , and the absolute difference between the two,  $|t_j - \tau_{crit,j}|$ , are calculated for each data point  $j$  between 5 and 45. In b) the estimated parameters  $c_1$ ,  $c_2$ ,  $c_3$ , and  $c_4$  are expressed as fractions of the optimal value for each parameter,  $c_{i,opt}$ . In c) cumulative infiltration is modelled using Eq.(4) with the optimal set of parameters; the white dot shows the transition time.



a)

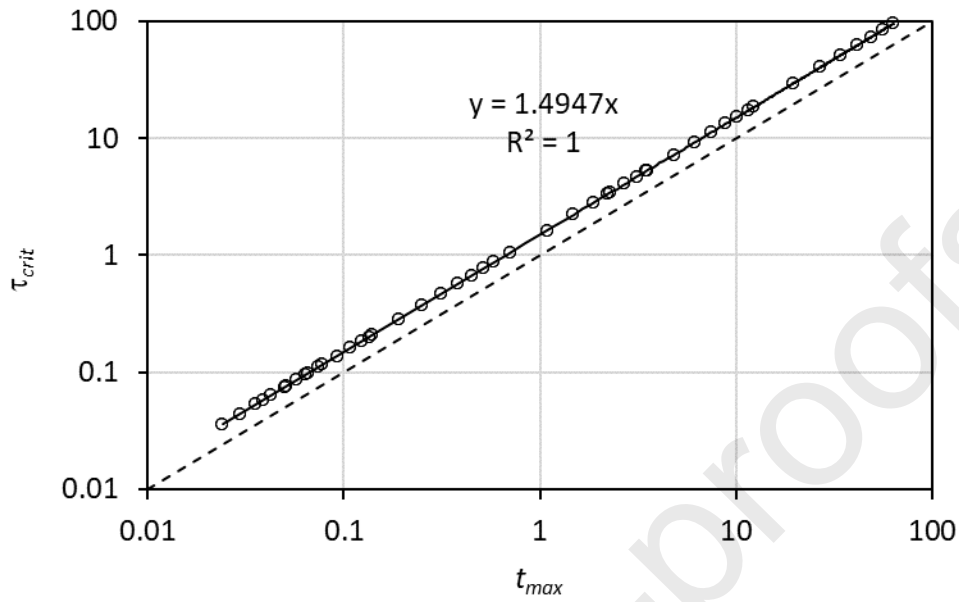


b)

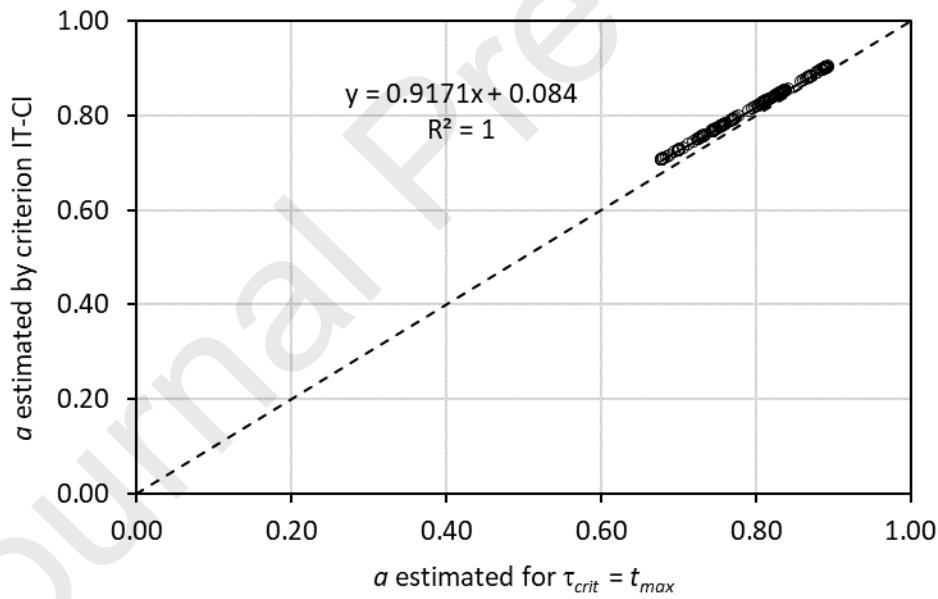


c)

822 **Figure 2.** Comparison between a) transition time  $\tau_{crit}$  and maximum time  $t_{max}$  for the analytically  
 823 generated infiltration experiments; b) values of  $a$  constant estimated by the iterative criterion IT-CI  
 824 and assuming  $\tau_{crit} = t_{max}$   
 825

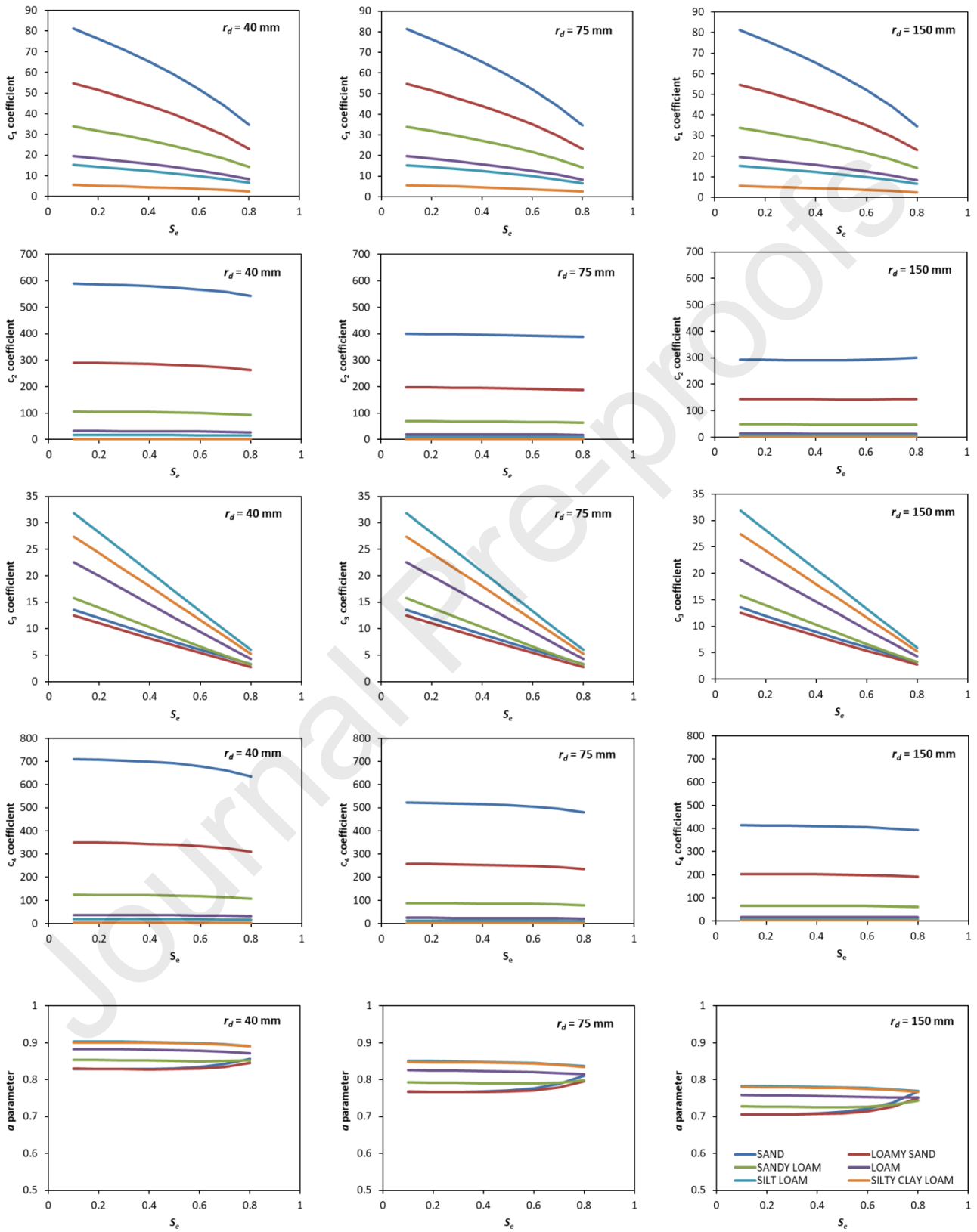


a)

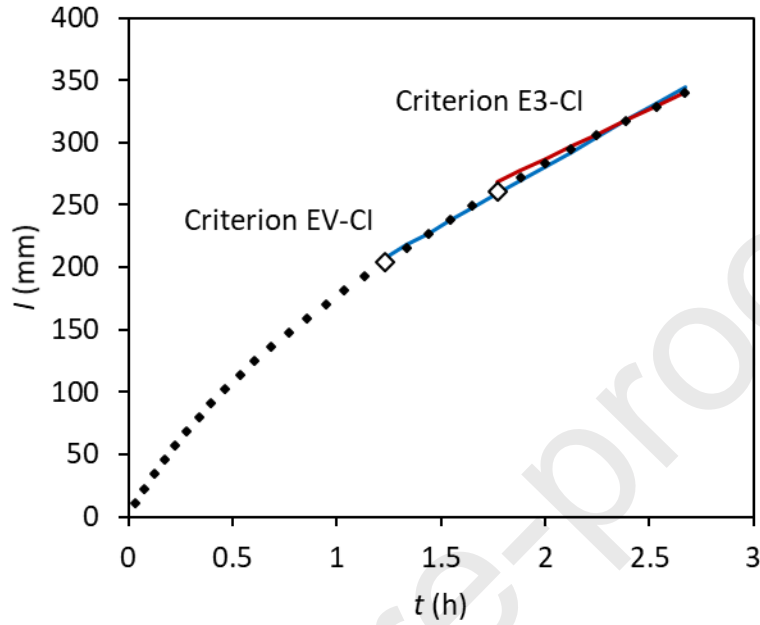


b)

**Figure 3.** Optimized values of infiltration coefficients  $c_1$ ,  $c_2$ ,  $c_3$  and  $c_4$  and  $a$  parameter as a function of initial degree of saturation,  $S_e$ , obtained for each soil and ring radius,  $r_d$ , by the iterative criterion IT-CI applied to analytically generated infiltration data.



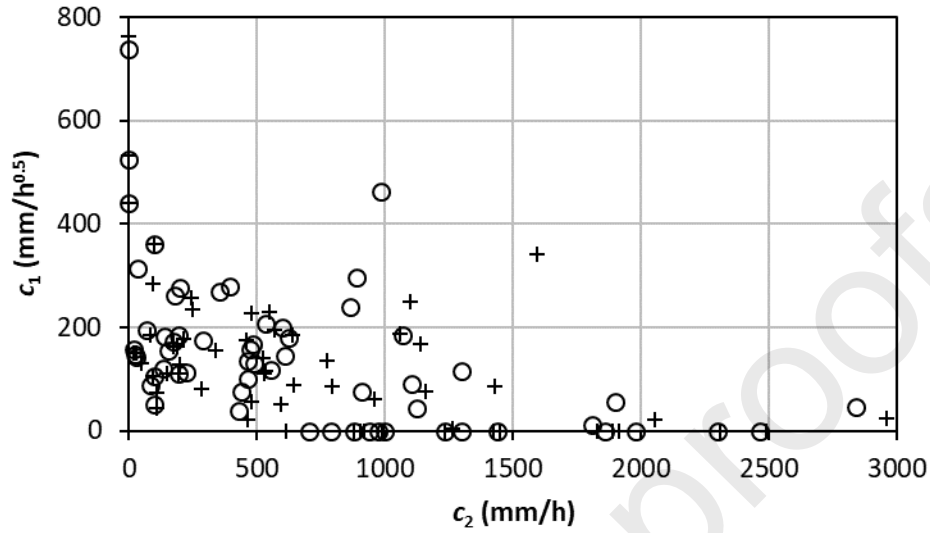
840 **Figure 4.** Example of  $\tau_{crit}$  estimation by different approaches for identifying the steady-state stage  
 841 of the infiltration process. Criterion E3-CI considers regression line fitting the last three data points.  
 842 Criterion EV-CI considers regression line fitting the whole set of cumulative infiltration data for  
 843 which  $\hat{E} \leq 2\%$  (Eq.(14)).  
 844  
 845



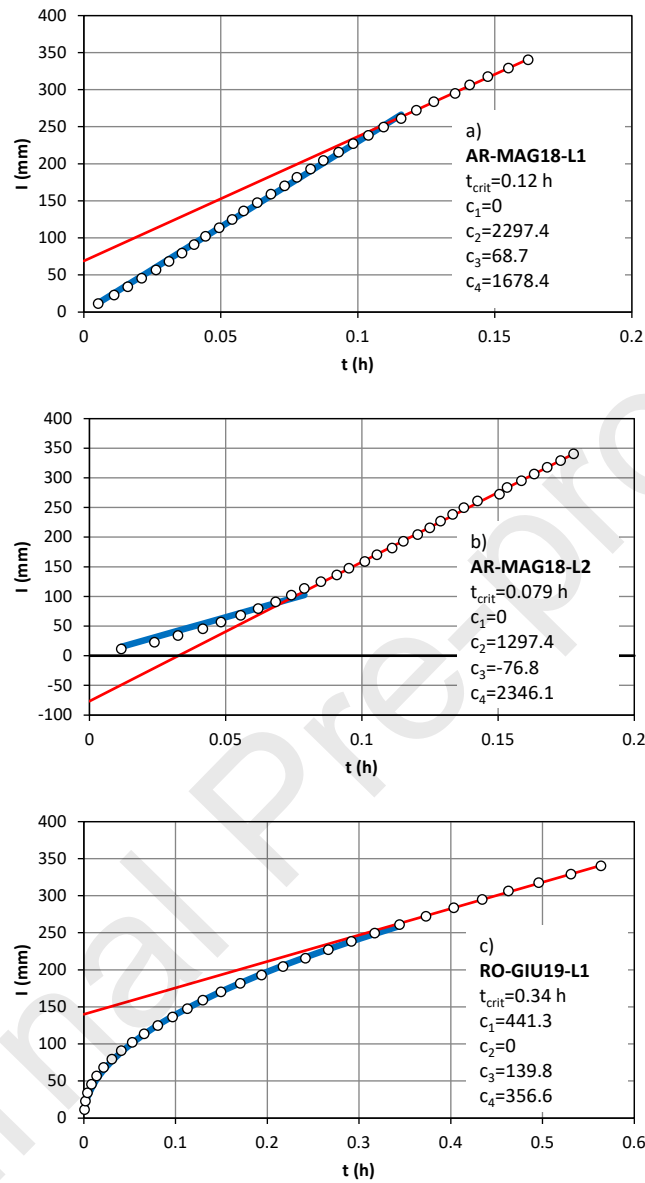
846

847

848 **Figure 5.** Scatter plot of the  $c_1$  vs.  $c_2$  coefficients estimated by criteria EV-CI (crosses) and E3-CI  
 849 (circles). (sample size,  $N = 60$ )

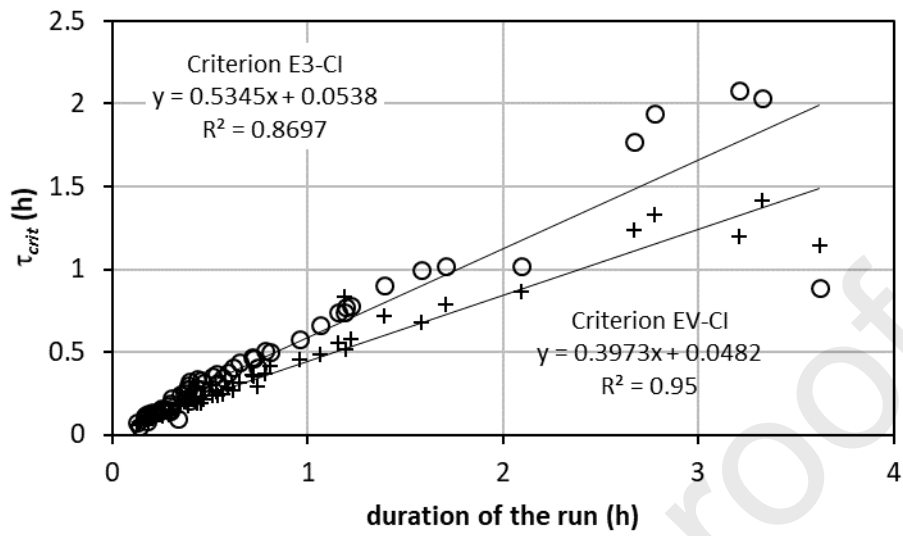


857 **Figure 6.** Examples of unsuccessful runs: a)  $c_1 = 0$ ; b)  $c_1 = 0$  and  $c_3 < 0$ ; and c)  $c_2 = 0$ . Blue lines  
 858 indicate the fitting of the transient model to the data and red lines indicate the adaption of the  
 859 steady-state model to the data  
 860



861  
 862

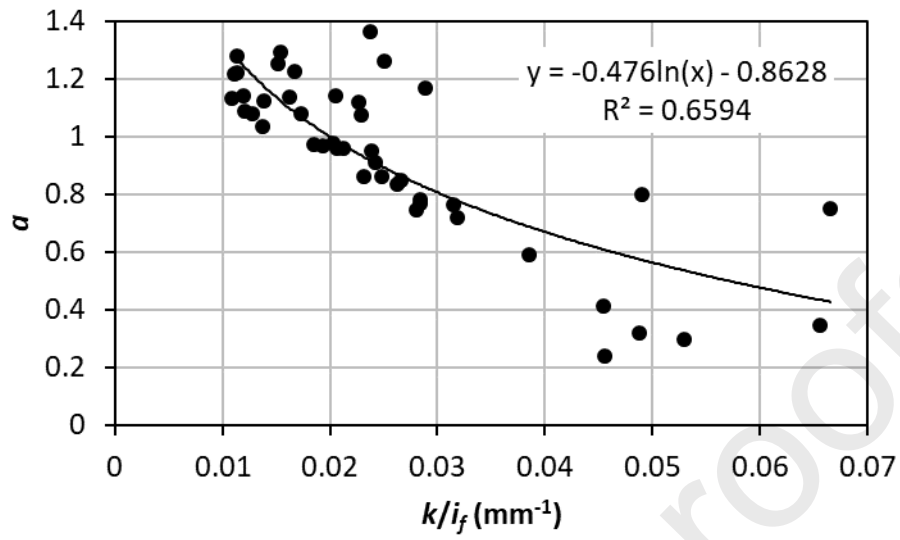
863 **Figure 7** Relationship between the total duration of the field run and the  $\tau_{crit}$  time estimated by  
 864 criteria EV-CI (crosses) and E3-CI (circles). (sample size,  $N = 60$ )  
 865



866  
 867



868 **Figure 8.** Relationship between the estimated  $a$  parameter and the normalized  $k$  constant of the  
 869 Horton infiltration model  
 870



871

872

873 MI: Conceptualization, Methodology, Investigation, Writing - original draft, Supervision. MAN:  
874 Conceptualization, Methodology, Formal analysis, Writing - Review & Editing. RAJ: Validation, Formal  
875 analysis, Writing - Review & Editing. VB: Conceptualization, Methodology, Investigation, Writing - original  
876 draft. MC: Data curation, Writing - Review & Editing. PC: Investigation, Writing - Review & Editing. SDP:  
877 Data curation, Writing - Review & Editing. LL: Conceptualization, Methodology, Formal analysis, Writing -  
878 Review & Editing, Supervision. RDS: Conceptualization, Methodology, Formal analysis, Writing - Review &  
879 Editing, Supervision.

880

881

882 **HIGHLIGHTS**

- 883 • A novel iterative method was proposed to estimate  $\tau_{crit}$  and  $a$  terms of SA model
- 884 • The  $a$  term is not a constant and can plausibly vary over the  $0.47 < a < 1$  range
- 885 • Fitted  $a$  values outside that range can indicate non-ideal infiltration conditions
- 886 • Uncertainty in the estimates of  $\tau_{crit}$  does not impact estimations of  $a$
- 887 • Appropriately constraining  $\tau_{crit}$  and  $a$  can improve accuracy of  $K_s$  estimates

888

889

890

891

**Declaration of interests**

☒ The authors declare that they have no known competing financial interests or personal relationships that could have appeared to influence the work reported in this paper.

☐ The authors declare the following financial interests/personal relationships which may be considered as potential competing interests:

